Study of the long time relaxation of the weak ferroelectricity in PbZrO 3 antiferroelectric thin film using Positive Up Negative Down and First Order Reversal Curves measurements

Kevin Nadaud, Caroline Borderon, Raphaël Renoud, Micka Bah, Stephane Ginestar, Hartmut Gundel

Study of the long time relaxation of the weak ferroelectricity in $PbZrO_3$ antiferroelectric thin film using Positive Up Negative Down and First Order Reversal Curves measurements

Kevin Nadaud[a,*], Caroline Borderon[b], Raphaël Renoud[b], Micka Bah[a], Stephane Ginestar[b], Hartmut W. Gundel[b]

[a]*GREMAN UMR 7347, Université de Tours, CNRS, INSA-CVL, 16 rue Pierre et Marie Curie, 37071 Tours, France*

[b]*Nantes Université, CNRS, IETR UMR 6164, 44000 Nantes, France*

Abstract

The weak ferroelectric contribution to the polarization of antiferroelectric lead zirconate (PZO) thin films has been investigated using PUND (Positive Up Negative Down) pulse measurements and hysterons decomposition by First Order Reversal Curves (FORC) technique. The PUND allows decomposing the measured current, obtained from the polarization-electric field loop measurements, into a switching and a non-switching contribution. We show that the weak ferroelectric phase is enhanced when a large electric field has been previously applied to the material, in order to switch from the antiferroelectric to the ferroelectric phase. Using the PUND measurement at fields below the antiferroelectric to ferroelectric phase transition, the polarization loop corresponding only to the ferroelectric switching contribution has been determined revealing that this contribution to the overall polarization is small. FORC measurements, however, indicate that the ferroelectric phase is present at different fields. At low fields, a quite homogeneous distribution of hysterons exists and at large field, a high concentration of hysterons at a field near to the antiferroelectric to ferroelectric phase transition can be seen. Moreover, when changing the delay between pulses of the PUND and the FORC measurements, we show that this weak ferroelectricity contribution is metastable and decreases with time.

Keywords: Anti-ferroelectric; Thin film; Residual ferroelectricity; Positive up negative

down pulse; First order reversal curves technique; Relaxation

1. Introduction

Antiferroelectric materials present an important interest for energy storage applications [1–3] due to the double hysteresis in the polarization versus electric field loop. When a high electric field is applied to an antiferroelectric material, a large increase of the polarization is obtained at the antiferroelectric (AFE) to ferroelectric (FE) phase transition, which permits a much higher stored energy compared to the case of linear dielectrics or relaxor ferroelectrics like $(1-x)Pb(Mg_{1/3}Nb_{2/3})O_3 - x\,PbTiO_3$[4]. Compared to hard ferroelectrics ($PbZrTiO_3$) a better efficiency due to a considerably larger released energy can be obtained. In antiferroelectric materials, however, a residual ferroelectric contribution, called weak ferroelectricity, may be present which increases the overall material's losses. This has been largely mentioned in the literature and widely studied using various methods such as low field hysteresis measurement [5–7] or impedance spectroscopy [8–10]. Understanding the influence of the residual ferroelectric phase of antiferroelectrics is mandatory in order to increase the stored energy and the efficiency of the AFE energy storage devices.

Pulse switching of ferroelectric materials has been described by Merz [11] in the fifties of the last century, especially in order to show the stable or not stable partial switching behavior of those materials. Also called PUND (Positive Up Negative Down) method [3, 12–14], and when applied to antiferroelectrics, this technique allows detecting a possible residual ferroelectric phase in the AFE material.

An initial pulse (here of negative polarity, rectangular, trapezoidal or triangular) is applied in order to switch all existing ferroelectric domains in a given direction (Fig. 1a). Then, two pulses of opposite polarity (P and U, here positive) are successively applied

*Corresponding author, Tel.: +33 247 366 947 ; fax: +33 247 367 121.
Email address: kevin.nadaud@univ-tours.fr (Kevin Nadaud)

and finally, the application of the pulses N and D, again of opposite polarity (here negative) allows obtaining the full hysteresis cycle. The current signal of the respective pulses is recorded.

In the case of the pulses P and N (so-called switching pulses), the measured current is the sum of the contributions (i) leakage current, (ii) capacitive charging,(iii) possible ferroelectric phase switching as the previous pulse was of opposite polarity, and (iv) polarization changes for fields higher than the AFE-FE phase transition field. In the case of a purely capacitive behavior, a triangular applied voltage should result in a constant current: positive if the voltage is increasing and negative if the voltage is decreasing. A deviation of this behavior indicates a polarization change at this particular field, which may include FE switching and AFE-FE phase transition depending on the field amplitude. The example of the current signals obtained for fields below the AFE-FE transition and for a small residual ferroelectric phase in the AFE material is shown in Fig. 1b, which can be used for representing the obtained global $I(E)$ cycle (Fig. 1c). For the pulses U and D (non switching pulses), no FE phase switching should occur as already switched by the previous pulses of the same polarity, and hence the current is the sum of only the three other contributions. By subtracting the non switching currents from the switching currents ($i_P - i_U$ and $i_N - i_D$), it is possible to extract the pure switching contribution for both polarities to compute the respective $I(E)$ loop (Fig. 1d).

In order to obtain a sufficient signal to noise ratio, the switching contribution needs to be high as compared to the capacitive and the leakage contributions. Otherwise, some current subtraction prior to the amplification and acquisition can be used [15]. This method has been widely used for ferroelectric materials in order to remove excessive capacitive and leakage contributions and to study the switching times of the different contribution to the polarization[3, 12–16] To the best of our knowledge, however, it has never been used for studying the weak ferroelectricity in antiferroelectrics.

Ferroelectric materials can also be investigated by First Order Reversal Curves (FORC) measurements which permit the decomposition of the $P(E)$ loop into elementary hysteresis contributions called hysterons [13, 17–20]. This method also gives information on the

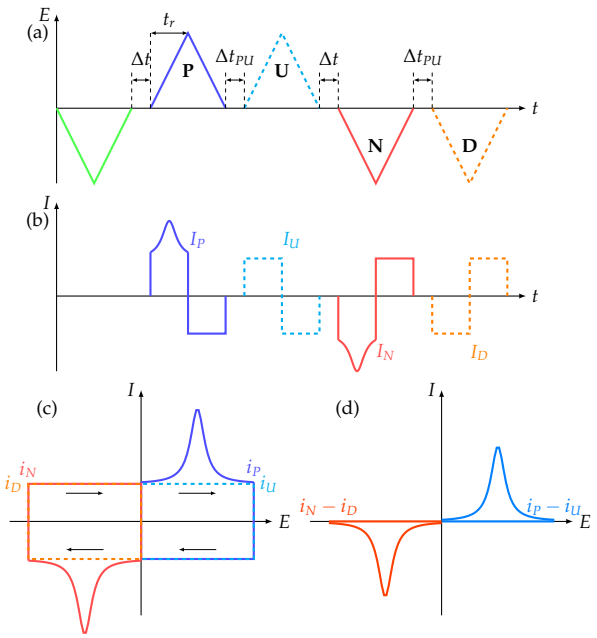

Figure 1: Applied PUND signal (a) and measured current (b), as function of time for fields below the AFE-FE transition. Global $I(E)$ cycle (c) and $I(E)$ cycle of only the ferroelectric switching contribution (d). t_r is the raise time of the pulse and Δt the delay between the orientation pulse and the PUND measurement, and Δt_{PU} the delay between the pulses P and U as well as N and D. Arrows indicates the sense of the cycle.

degradation of the material and the presence of a possible residual ferroelectric phase in AFE materials which otherwise is difficult to see from the $P(E)$ loops [8, 18, 21–23]. The standard implementation of this method is to vary the electric field from one saturation state to another[18–20] but it is also possible to use a bipolar waveform with an increasing amplitude[8, 24]. The advantage of the bipolar waveform approach is the existing delay between the different pulses allowing to investigate temporal relaxation of the switching processes which can reach several tens of second in ferroelectric [25] and in antiferroelectric [26, 27] materials.

In this paper, the complementary PUND and FORC measurements are used in order to obtain a better understanding of the weak ferroelectricity in antiferroelectric $PbZrO_3$, visible at low fields and to study especially its temporal relaxation and the dependence on the applied electric field amplitude. In the first part, conventional $P(E)$-loops (at low and large fields) are used in order to show the weak ferroelectric phase enhancement in the material after the realization of a $P(E)$ major loop. The ferroelectric switching

contribution to the polarization is studied by PUND measurements, for different amplitudes of the electric field and with different delay time between the pulses, in the second and third part, respectively. Using these measurements, the $P(E)$ loop of the switching contribution has been extracted in order to see the effect of amplitude and delay and to study the evolution of the antiferroelectric-ferroelectric transition fields. In the last part, FORC measurements are presented in order to gain better understanding of the phenomena that appear at low and high fields, and to correlate them to the results of the PUND measurements.

2. Experiments

Antiferroelectric lead zirconate ($PbZrO_3$) thin films are prepared by a sol-gel process using multi-step spin coating[1, 8, 9]. Firstly, lead acetate trihydrate [$Pb(CH_3CO_2)_2 \cdot 3\,H_2O$] is dissolved in de-ionized water and acetic acid. Zirconium isopropoxide [$Zr(O(CH_2)_2CH_3)_4$] is then added in the solution, as well as ethylene glycol [$HO-CH_2-CH_2-OH$] used for reducing the appearance of micro-cracks[28] in the films and improves the solution stability[29]. The solution has been deposited on alumina substrates precoated with a titanium and platinum layers in order to form the bottom electrode. Twelve layers result in an overall film thickness of 800 nm. Square platinum electrodes of 0.1 mm width are deposited by RF magnetron sputtering in order to realize a Metal-Insulator-Metal (MIM) capacitor and to allow the dielectric characterizations of the fabricated thin films. Structural characterizations reveal the studied thin film presents the (100) and (111) crystallographic orientations [1] and presents a columnar structure [8, 30].

The electric measurements have been performed with an AixACCT TF2000 ferroelectric analyzer. The conventional $P(E)$ loops, presented in the first part, have been measured using a sine waveform and the applied voltage has been varied from 2 V to 40 V with a step of 2 V. The AFE-FE transition fields correspond to the maxima of the respective current waveforms. In the case of the PUND pulse measurements, a triangular waveform with a voltage sweep from 10 V to 70 V, corresponding to an electric field from 125 kV cm^{-1} to 875 kV cm^{-1}, and a step of 10 V have been applied, with the sequence de-

scribed Fig. 1. The delay between the pulses Δt has been varied from 1 µs to 1000 s and the duration of the pulses $2t_r$ has been adjusted for a constant slew rate of 4 V ms^{-1}. For the construction of the $P(E)$ loops of the pure switching contribution, the non-switching current is subtracted from the switching current signal and integration as a function of time to obtain the polarization.

The waveform used for the FORC measurements correspond is similar to this PUND method, except that only the switching pulses P and N are applied. The delay between the positive and negative pulses has been varied from 1 µs to 1000 s and the duration of the pulse slew rate has been kept constant. The FORC distribution extraction method is presented elsewhere [8, 24]. The applied voltage has been swept from 2 V to 70 V with a step of 2 V corresponding to an electric field varying from 25 kV cm^{-1} to 875 kV cm^{-1}. Reduction of the step voltage permits increasing of FORC distribution resolution and hence to better discern the residual ferroelectric phase.

3. Results and discussions

In the first part, conventional $P(E)$ loops are presented in order to show the current peaks associated to the weak ferroelectricity in the studied PZO thin films. In the second and third parts, a precise characterization of this weak ferroelectricity has been done using the PUND method by varying respectively the electric field amplitude and the delay between pulses. Each time, the PUND measurements are presented separately for low and high fields. Finally, the FORC measurements are used in order to show the effect of the delay between pulses on the high field ferroelectric contribution.

3.1. Large field $P(E)$ loops

The polarization has been measured as a function of voltage with an amplitude swept from 2 V to 70 V with a step of 2 V, corresponding to an electric field of 25 kV cm^{-1} and 875 kV cm^{-1} applied to the 800 nm thick sample.

The polarization versus electric field loops obtained from a virgin sample are shown in Fig. 2a. The typical double hysteresis of an antiferroelectric material is well visible. The maximum value of polarization is 26 µC cm^{-2} which is close to the value reported

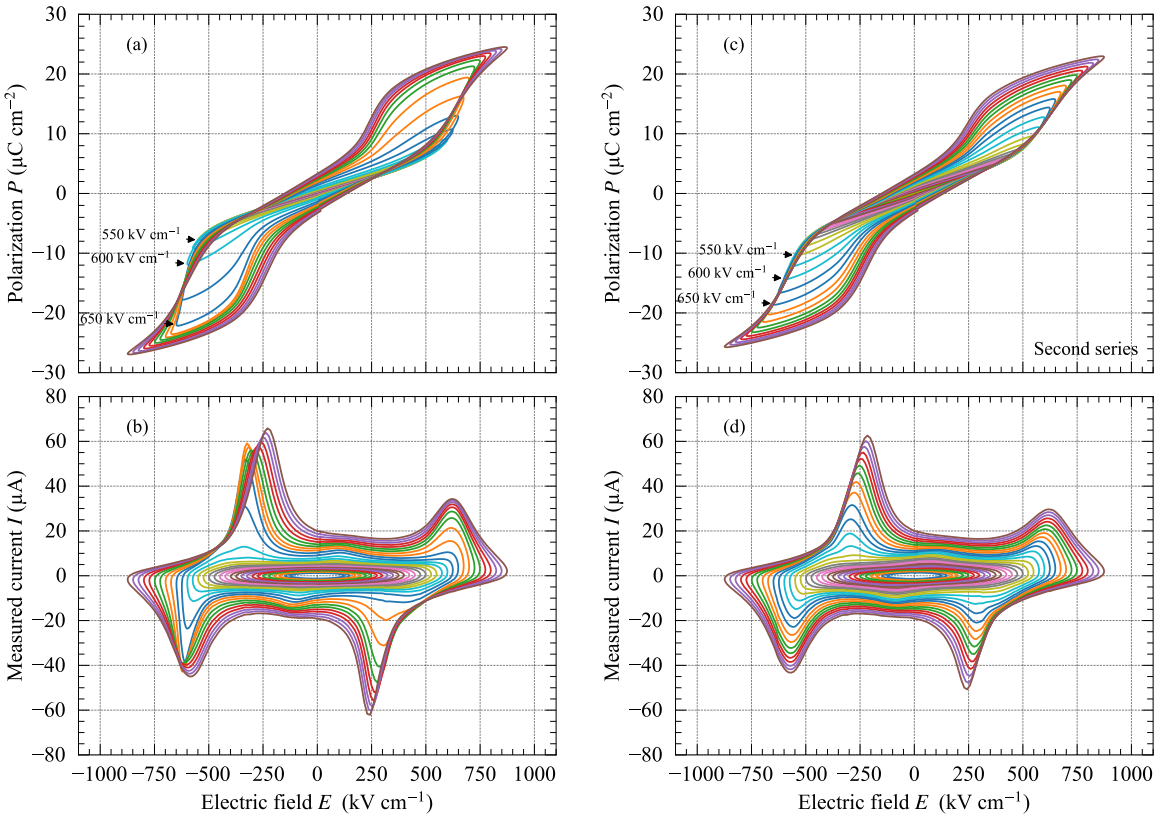

Figure 2: $P(E)$ loops of the first (a) and second (b) series of cycles and corresponding current of the first (c) and second (d) series.

for PZO thin films [31]. The antiferroelectric to ferroelectric and ferroelectric to antiferroelectric transition fields are respectively $E_{AF}^{+} = 628\,\mathrm{kV\,cm^{-1}}$ and $E_{FA}^{+} = 244\,\mathrm{kV\,cm^{-1}}$ for the positive and $E_{AF}^{-} = -580\,\mathrm{kV\,cm^{-1}}$ and $E_{FA}^{-} = -229\,\mathrm{kV\,cm^{-1}}$ for the negative polarity. In the case of this first measurement, the significant increase of the polarization is visible at field above $\pm 575\,\mathrm{kV\,cm^{-1}}$, indicating the onset of a rapid antiferroelectric to ferroelectric phase transition. The current loops corresponding to these first applied electric fields cycles are shown Fig. 2c When repeating the measurement for a second time, similar values of the maximum polarization and transition fields are obtained (Fig. 2b), however, the curves are more regularly spaced and the sharp increase of the polarization at driving fields between $575\,\mathrm{kV\,cm^{-1}}$ and $650\,\mathrm{kV\,cm^{-1}}$ is not visible (Fig. 2d). This difference is attributed to the enhanced weak ferroelectricity and will be detailed below, discussing

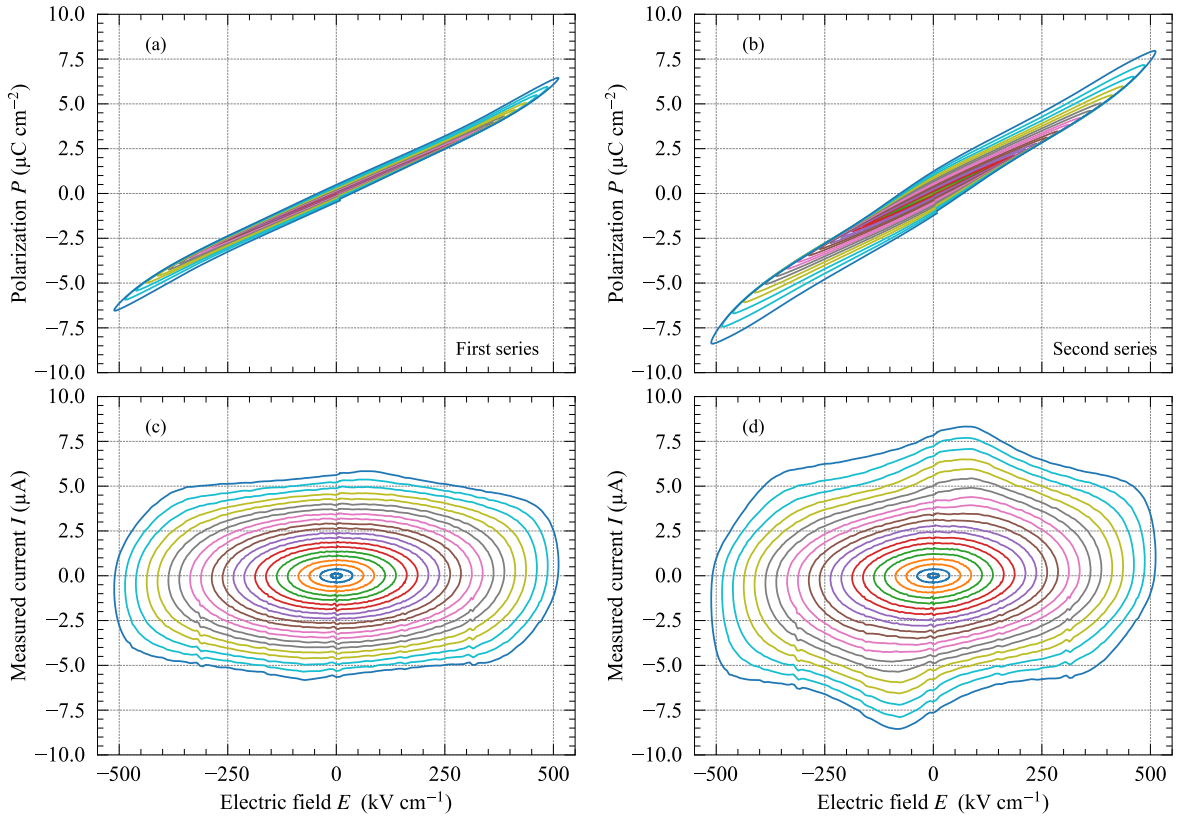

Figure 3: Polarization (a)(b) and current (c)(d) for the first series of measurement (a)(c) and for the second series of measurement, after a major loop with a driving field amplitude of 875 kV cm^{-1} (b)(d).

the low field $P(E)$-loops.

3.2. *Low fields $P(E)$-loops*

The polarization and current loops of Fig. 2 for electric fields below 500 kV cm^{-1} are shown in Fig. 3a and 3c for the first applied cycles (i.e. new sample) and in Fig. 3b and 3d for the second cycles (i.e. after the exposition of the sample to the maximum electric field of 875 kV cm^{-1}). At low electric fields, and especially for the first applied cycles (Fig. 3c), the current describes an ellipse with the principal axis near to the x-axis, which is typical for a capacitive behavior when using a sinewave excitation and indicates a low leakage current. In the case of the cycles after a major loop with a driving field amplitude of 875 kV cm^{-1} had been applied, a more open $P(E)$ loop, (Fig. 3b) and a current peak at $\pm$100 kV cm^{-1} (3d) are observed, less visible but already existing for the

first cycles. This current peak is attributed to the weak ferroelectric contribution [5–7] in the AFE thin film. This indicates that the ferroelectricity is present into the material, even before the application of the large electric field of $875\,\mathrm{kV\,cm^{-1}}$ and is largely enhanced by the application of a large electric field. The opening of the $P(E)$-loops in the case of the second series indicates higher losses, which can be attributed to the more important switching contribution.

For certain compounds of PZO-based antiferroelectric materials [32–36], the whole material stays in the ferroelectric phase when the electric field applied during the initial AFE-FE phase transition is released, and the transition is hence irreversible. In our case, the phase transition is reversible and the major part of material goes back to the antiferroelectric phase, giving rise to the typical double hysteresis loop. One part of the material, however, stays in the ferroelectric phase thus enhancing the weak ferroelectricity.

One can note that the weak ferroelectricity is only visible around $E = \pm 100\,\mathrm{kV\,cm^{-1}}$ if a larger electric field is applied during the cycle. This suggests that the weak ferroelectricity switching depends on the electric field amplitude previously applied and has a time relaxation.

In order to better study the influence of the weak ferroelectric contribution to the overall properties, the PUND method has been used which allow separating the switching and the non-switching contributions. To begin with (section 3.3), the measurements have been done for different electric field amplitudes and a given delay between pulses to determine the minimum electric field necessary to enhance the weak ferroelectricity. After that, the delay between the pulses has been varied in order to discern stable and unstable ferroelectric switching (section 3.4).

3.3. PUND measurement with fixed delay between pulses

To begin with, the delay Δt between the negative orientation pulse and the PUND measurements as well as the delay Δt_{PU} between the PUND pulses has been set to 250 µs. The measured current is plotted as a function of the electric field for fields below the AFE-FE phase transition field ($E_{max} \leq 500\,\mathrm{kV\,cm^{-1}}$) and for fields above ($E_{max} > 500\,\mathrm{kV\,cm^{-1}}$)

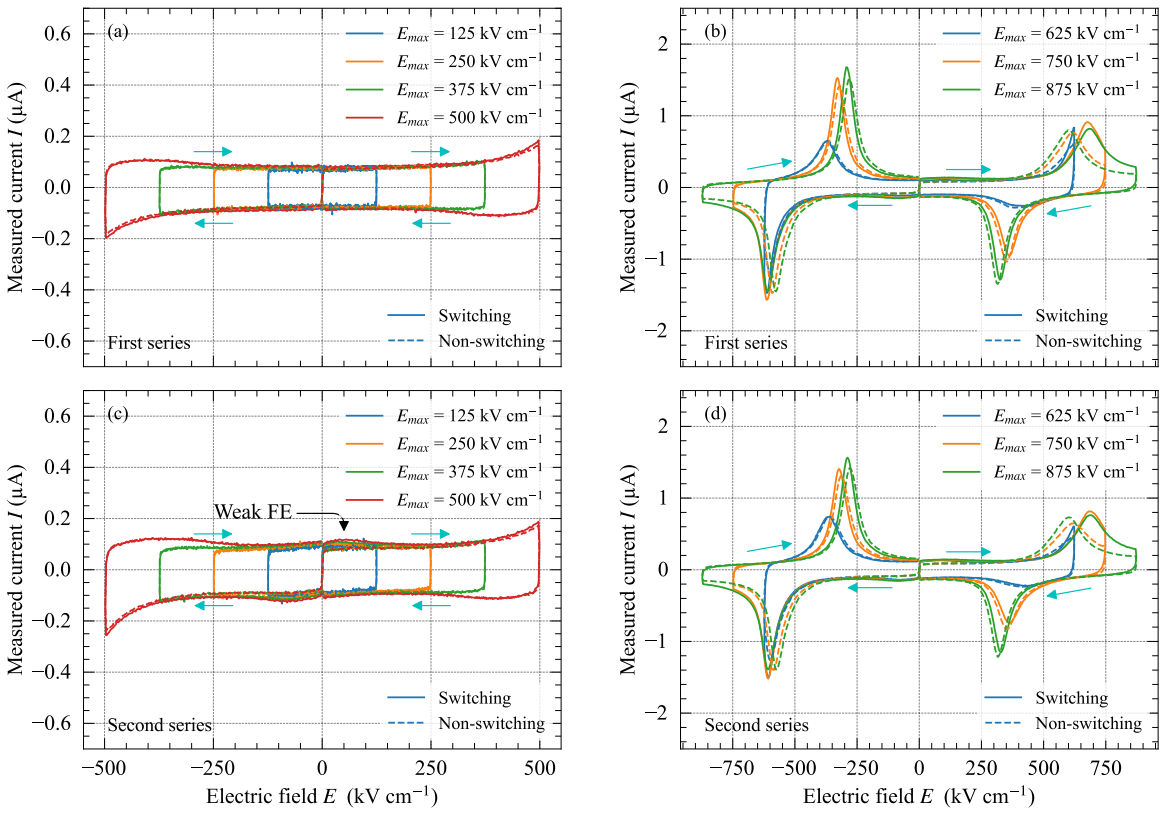

Figure 4: PUND current measurements as a function of the applied electric field of the first series (a),(b) and of the second series (c),(d). For fields below (a),(c) and above (b),(d) the AFE-FE phase transition. The switching pulses are shown in full line and the non-switching pulses in dashed lines.

in Figs 4a and 4c and Figs. 4b and 4d, respectively.

Below the AFE-FE phase transition and in the case of the first series of applied fields, no notable difference between the switching and the non switching current is visible (Fig. 4a) suggesting that switching of the residual ferroelectric phase does not occur. At electric fields above the AFE-FE phase transition (Fig. 4b), the switching current exceeds the non switching current, well visible for the highest applied fields. In the case of the second series, even below the phase transition, a small difference between the switching and the non switching current appears, visible around $\pm 100\,\mathrm{kV\,cm^{-1}}$ (Fig. 4c). The broad current peak indicates that there does not exist a sharp but a rather distributed coercive field.

For fields above the AFE-FE transition, switching of the ferroelectric residual phase

is hardly visible due to the much more important amplitude of the phase transition current. There is no significant difference between the first and the second measurement series since, for field above the AFE-FE transition, the sample has already been exposed to a large field and changes the phase structure of the material (a part of the material stays in the ferroelectric phase). For both series, the maximum of the phase transition current appears at higher fields for the switching pulses, particularly well visible in the case of the positive pulses P and U (after initial orientation by application of a negative pulse). The shift of the current maximum is 100 kV cm^{-1} (from 700 kV cm^{-1} to 600 kV cm^{-1}) for the E_{AF}^{+} field and 35 kV cm^{-1} for the E_{AF}^{-} field while small for the ferroelectric to antiferroelectric transitions E_{FA}^{+} (below 10 kV cm^{-1}). The antiferroelectric to ferroelectric transition hence seems to depend on the initial polarization orientation of the material, which correspond to a memory effect in antiferroelectric materials [37]. The residual ferroelectric cells that switch below the antiferroelectric to ferroelectric transition [8] may also influence and thus lower the transition field when initially orientated favorably.

3.4. Influence of the delay between the pulses of the PUND measurement

In the previous section, the delay between pulses has been kept constant (250 µs). The delay between the initial orientation pulse and the PUND measurement pulses however influences the switching behavior. We have hence varied this delay from 1 µs to 1000 s using a homogeneous repartition in the logarithmic scale. All measurements presented in this section have been performed on an enhanced ferroelectric behavior sample that has already been exposed to an electric field of 875 kV cm^{-1}. As before, we study (i) ferroelectric switching at low fields and (ii) the AFE-FE transition at high fields.

3.4.1. Low field measurements

The full switching and non switching current waveforms for different delay are shown in Fig. 5a and 5b, respectively for a field of 500 kV cm^{-1}. The non switching current almost does not depend on the delay Δt_{PU} between the pulses P and U, although it is possible to subtract the non-switching from the switching current in order to amplify the difference.

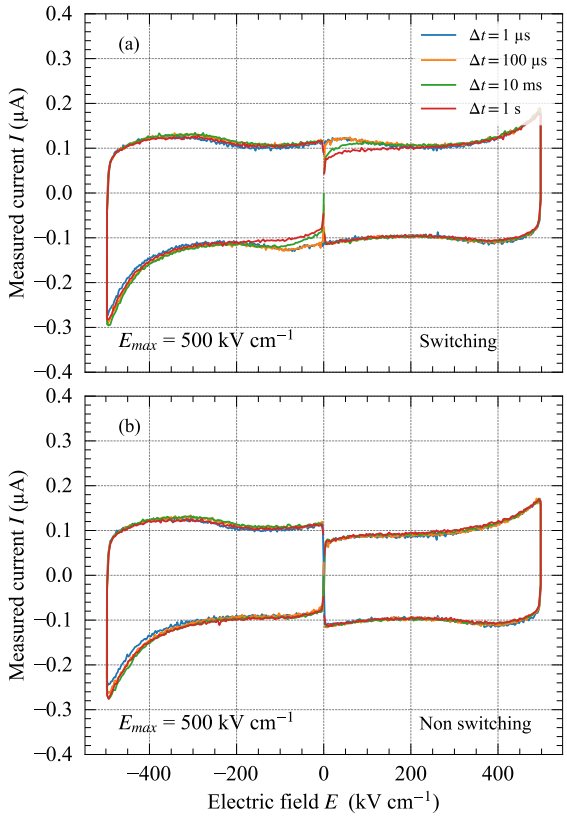

Figure 5: Measured switching current (a) and non switching current (b), at 500 kV cm^{-1}, for various delay Δt_{PU} between the pulses P and U as well as N and D of the PUND measurement.

The differential current waveforms for various delay times Δt between the initial orientation pulse and the PUND measurement pulses and for different applied field are shown in Fig. 6. As the delay between the orientation pulse and the PUND measurement evolves, the differential current signal changes, showing that the orientation of the residual ferroelectric phase is not stable. Independent of the applied field, a maximum of polarization switching is obtained for delay times $\Delta t \leq 100\,\mu s$. As the delay is getting longer, the differential switching current signal decreases, indicating a partial relaxation of the initial domain orientation. For delay times longer than 100 s, the differential current signal disappears. This indicates that the influence of the negative orientation pulse prior to the PUND measurements has become negligible and that the ferroelectric domains are completely relaxed. A similar behavior has been observed for all applied electric fields.

Integration with time of the differential current waveform signals allows obtaining the $P(E)$ loop of the residual ferroelectric phase which is shown in Fig. 7a for a driving field amplitude of $500\,kV\,cm^{-1}$ and for different delay times Δt. The straight horizontal lines of the $P(E)$ cycles when the applied field decreases to zero are typical for corrected PUND loops[12, 14].

The maximum value of the weak ferroelectric contribution $P = 0.7\,\mu C\,cm^{-2}$ for a field $E_{max} = 500\,kV\,cm^{-1}$ is very small compared to the typical values of polarization for ferroelectric or antiferroelectric materials. In accordance to the broad current peaks of Fig. 6, a rather wide distribution of the coercive field (with a mean value around $150\,kV\,cm^{-1}$) has been found, confirming the poly-crystalline structure of the thin film.

The difference between the maximum and the minimum polarization, ΔP_m has been calculated for each delay time between pulses and is reported on Fig. 7b, showing that the switched polarization depends on the delay between the orientation pulse and the PUND measurement. At shortest delay times Δt, the switched polarization slightly increases and achieves a maximum value for several tens of microseconds. Complete switching of the residual ferroelectric phase hence can be supposed at the maxima of the respective polarization versus delay curves of Fig. 7b. For further increasing delay, however, the switched polarization ΔP_m decreases and tends to zero at delay times of the order of

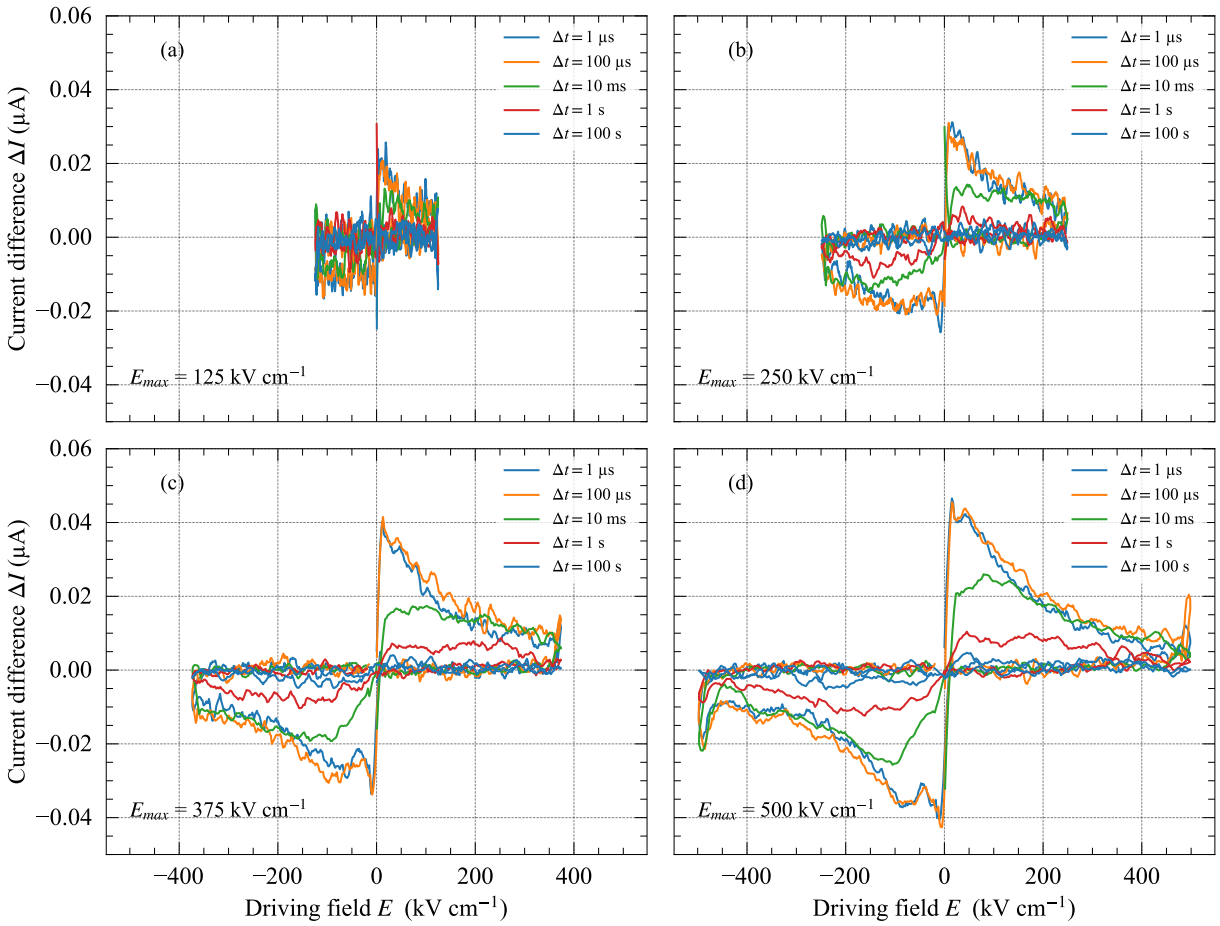

Figure 6: Differential current waveforms $I_{SW} - I_{NS}$ for different applied fields and various delay times Δt between the negative orientation pulse and the PUND measurements.

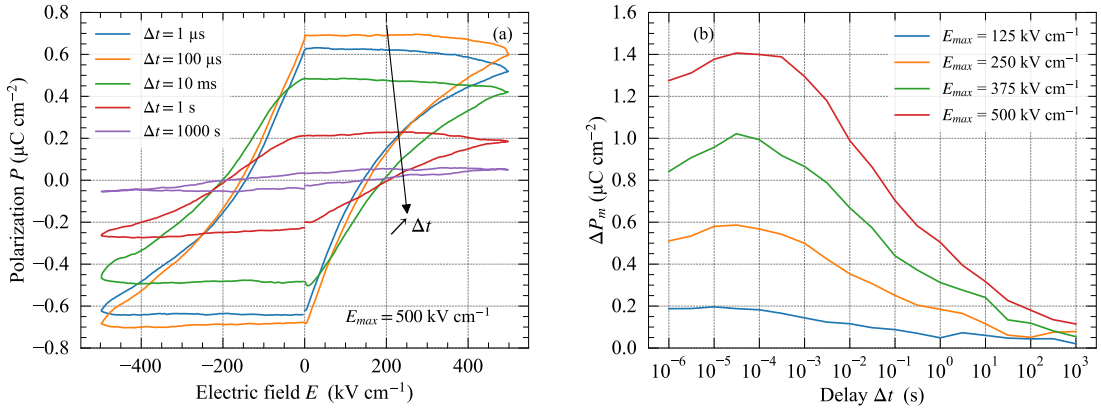

Figure 7: Reconstructed $P(E)$ loops concerning only the switching contribution for difference value of the delay between pulses and for a maximum electric field of 500 kV cm^{-1} (a). Difference between maximum and minimum polarization as a function of the delay between pulses for the reconstructed $P(E)$ loops (b).

several seconds, indicating that the orientation of the weak ferroelectricity is not stable. The existence of small ferroelectric clusters in antiferroelectric materials has been shown previously[8, 9], the dimension of those ferroelectric domains however seems to be too small in order to allow self-maintaining of oriented polarization. The mean coercive field value increases with increasing delay Δt indicating that the ferroelectric cells which do not go back to the antiferroelectric phase need a higher electric field to switch. The polycrystalline structure of the film and the small grain size create different local clamping conditions for each ferroelectric cluster. Each ferroelectric cluster thus has a different polar orientation with respect to the electric field and surrounding environment implying a distribution of coercive field and delay to go back to the antiferroelectric phase.

3.4.2. High field measurements

The current as a function of an applied electric field above $625\,\mathrm{kV\,cm^{-1}}$ is shown in Fig. 8 for various delay times between the orientation pulse and the PUND measurement. While successive application of the two positive P and U pulses should result in an identical phase transition current, it can be more particularly noticed that the phase transition field E_{AF}^{+} is approximately $100\,\mathrm{kV\,cm^{-1}}$ higher for the P-pulse (switching pulse), especially when the delay time Δt is short (Fig. 8a). This difference decreases with increasing delay Δt and disappears at longest delay times (Fig. 8d). Only a much smaller difference (around $30\,\mathrm{kV\,cm^{-1}}$) of the phase transition field E_{AF}^{-} between the respective N and D pulse is observed. The ferroelectric to antiferroelectric relaxation (field E_{AF}^{-}) seems not to be affected, neither by the type of pulse (switching or non-switching) nor by the delay Δt.

As shown in Fig. 7, switching of the residual ferroelectric phase at low fields is visible. The electric field amplitude does not increase the low field switching current, indicating that the ferroelectric phase can be fully orientated already by the fields employed for the low field measurements. As already seen before, increasing of the delay time Δt leads to less switching of the residual ferroelectric phase.

For a better visibility, the phase transition fields E_{AF} and E_{FA} have been extracted for each delay Δt and are reported Fig. 9. For a delay times between pulses between up to

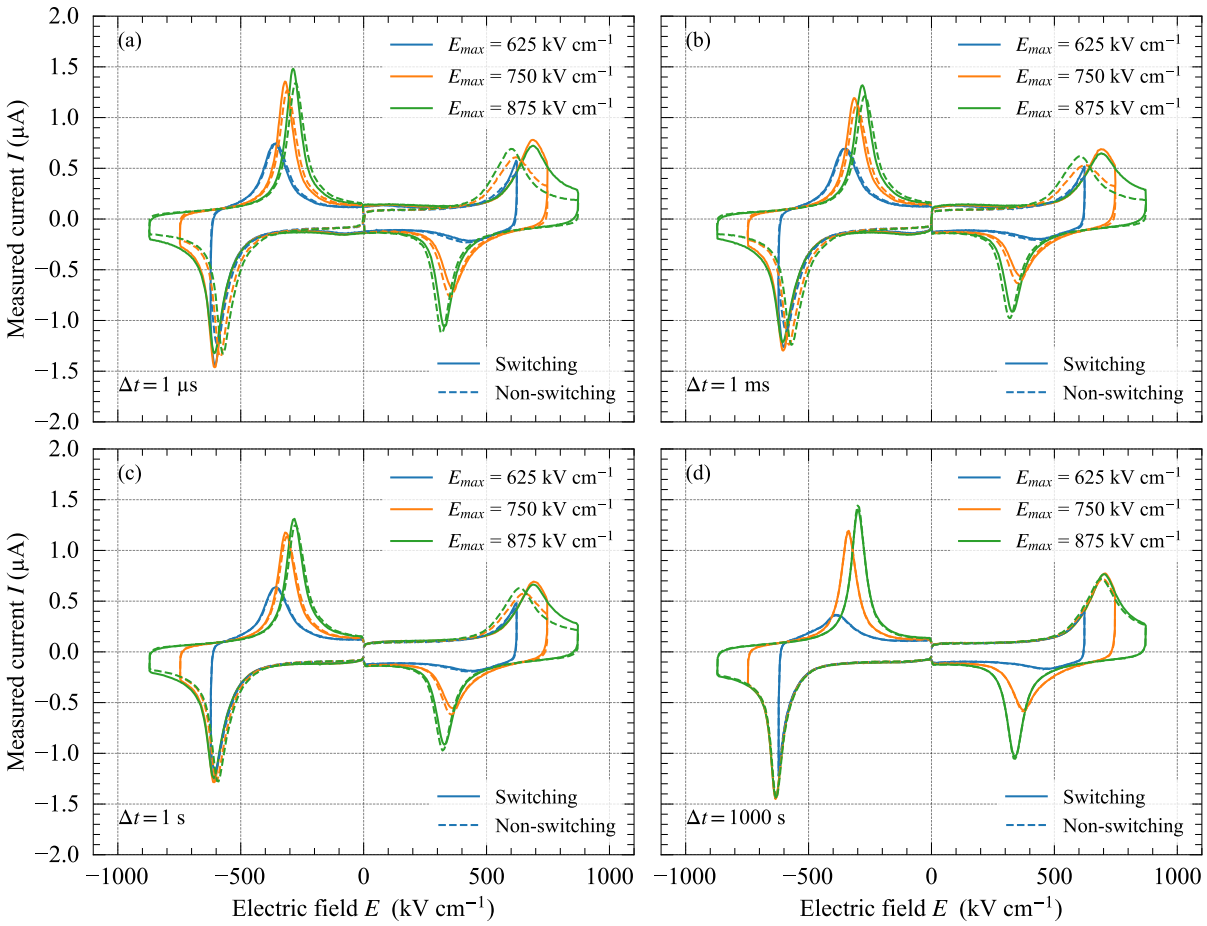

Figure 8: Measured current as a function of the applied electric field for the PUND measurement for various delay times between pulses, for electric field above 625 kV cm^{-1}. Switching pulses are in full line and non-switching pulses are in dashed lines.

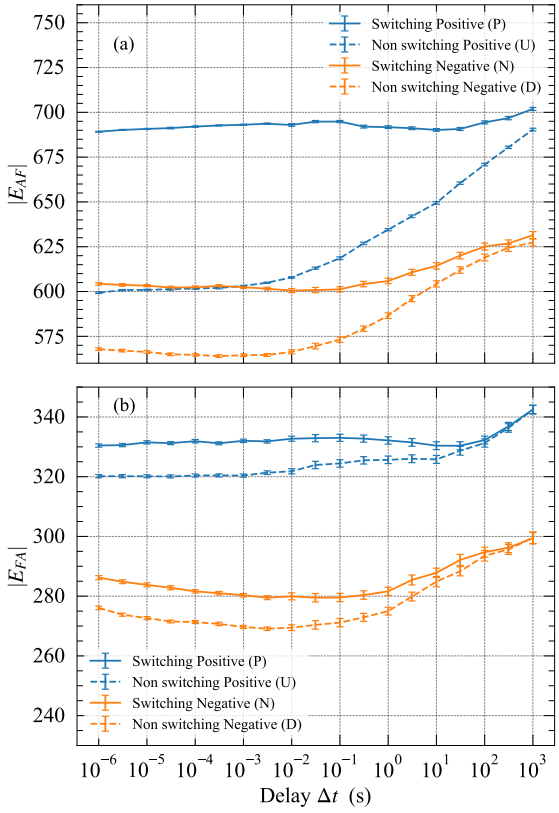

Figure 9: AFE-FE (a) and FE-AFE (b) transition fields as a function of the delay Δt for switching and non-switching pulses of positive and negative polarity obtained by PUND measurement.

several milliseconds, the transition fields are rather constant and the difference between switching and non-switching is well visible, with an antiferroelectric to ferroelectric transition field which is $90\,\mathrm{kV\,cm^{-1}}$ higher for the positive pulse and $35\,\mathrm{kV\,cm^{-1}}$ higher for the negative pulse. The difference of the ferroelectric to antiferroelectric transition fields is much smaller (about $10\,\mathrm{kV\,cm^{-1}}$) and does not depend on the polarity of the pulses. An asymmetry of the switching and non-switching transition fields has already been reported for $Pb_{0.99}Nb_{0.02}[(Zr_{0.6}Sn_{0.4})_{0.95}Ti_{0.05}]_{0.98}O_3$ ceramics [37]. In the present case, the observed asymmetry also may come from the asymmetry of the sample, i.e. the number of annealing steps for each layer. The last layer has been annealed only one time wheres the first one has been annealed twelve times and the following layers have a successively decreasing number of heat treatments. Annealing in air atmosphere may create oxygen vacancies in the structure which are known to be responsible of imprint and internal bias for ferroelectric materials [38, 39].

For a delay between pulses above several milliseconds, the difference between the switching and the non-switching transition field progressively weakens due to an increase of the non-switching field, while the switching field rather remains constant. Similar to what has been observed for the switching of the weak ferroelectric phase, the transition between the antiferroelectric and the ferroelectric phase is influenced by the delay time Δt, too. Switching of the residual ferroelectric phase seems to lower the AFE-FE transition field for the successively applied pulse of the same polarity as long as the delay Δt is sufficiently short to maintain the orientation of the weak ferroelectricity. The AFE-FE transition is hence favored by the previous orientation of the residual ferroelectric phase. The influence of the delay Δt on the ferroelectric to antiferroelectric relaxation electric field is similar but less pronounced since switching of the ferroelectric phase already has be established by the first pulse (switching-pulse). The internal fields hence are less modified, also limiting the change of the AFE-FE relaxation electric field.

3.5. *FORC measurement*

In order to further study the ferroelectric contribution into the PZO thin film, FORC measurements with increasing delay time between the positive and the negative pulse have been done. The FORC distributions for various delay between the pulses are shown Fig. 10, the $P(E)$ loops which were used for the FORC extraction are given in the supplementary material. The two peaks visible at $(E; E_r) = (-350\,\mathrm{kV\,cm^{-1}}; -650\,\mathrm{kV\,cm^{-1}})$ and $(700\,\mathrm{kV\,cm^{-1}};\ 350\,\mathrm{kV\,cm^{-1}})$ correspond to the antiferroelectric-ferroelectric transitions. When the delay between pulses changes, the peaks keep its position and the respective intensity is only slightly affected. The width of the peaks is due to the distribution of the transitions fields.

Further to the phase transition peaks, an additional ferroelectric contribution is visible in the bottom-right corner of the FORC distribution at the position $(E; E_r) = (700\,\mathrm{kV\,cm^{-1}}; -650\,\mathrm{kV\,cm^{-1}})$, highlighted by the red arrow. This ferroelectric contribution can not be discerned by the high field PUND measurements because the switching current peaks occur for the same field than the antiferroelectric to ferroelectric transitions: for positive fields, the ferroelectric phase switches at $E^+ = 700\,\mathrm{kV\,cm^{-1}}$, same field than E^+_{AF} and for negative field, it switches at $E^- = -650\,\mathrm{kV\,cm^{-1}}$ same field than E^-_{AF}. Switching of this ferroelectric phase is correlated to the antiferroelectric phase transition [8] since the field values correspond to the sharp increases of the polarization which occurs for the first measurement series (See section 3.1 Large field $P(E)$ loops) and which is related to the irreversible antiferroelectric to ferroelectric transition. As the delay time between the pulses increases, the position of this ferroelectric contribution remains unchanged, the magnitude of the peaks, however, decreases and finally disappears, indicating relaxation with time of this contribution. This is consistent to what has been found from the high field PUND measurements and indicates that the difference between switching and non-switching transition fields is influenced by this high field ferroelectric contribution. The very sensitive FORC measurement technique allows evidencing this contribution although not visible from the $P(E)$ loop.

A more subtle evolution in the FORC distribution in area around the $E_r = -E$ axis

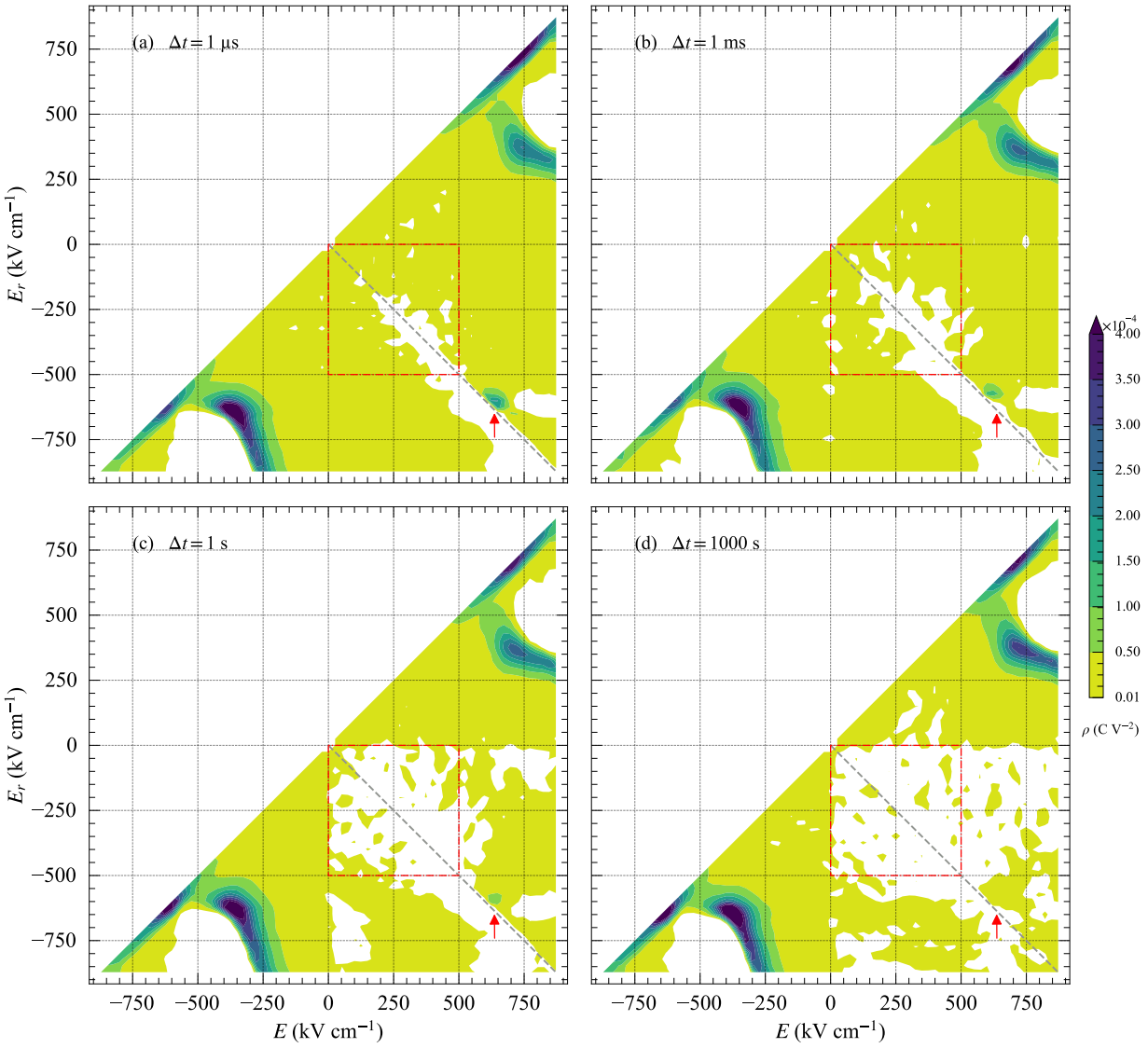

Figure 10: FORC distributions for different delay between the positive and the negative pulse. The dashed gray line shows the $E_r = -E$ axis. The red arrows point toward the position of the high field ferroelectric contribution peak and the red square indicates the low field hysterons. Density values below $1 \times 10^{-6}\,\mathrm{C\,V^{-2}}$ are displayed in white.

(dotted line in Fig. 10), delimited by the red square can be seen. When the delay between pulses increases, the hysteron density in this area progressively decreases, corresponding to a decrease of the switching polarization contribution studied in the low field section 3.4.1 (decrease of ΔP_m with time). In this area, a homogeneous low hysteron density is visible indicating that switching of the weak ferroelectric phase does not appear at a precise coercive field but with rather distributed values, as already seen from the broad current peak of Fig. 6.

4. Conclusion

In this paper, using the complementary PUND and FORC methods, we study the time and field dependency of the ferroelectricity contribution to the polarization in antiferroelectric PZO thin film. The PUND measurement permits us to show that some residual ferroelectric phase is present in the antiferroelectric thin film and can be switched at low fields. By varying the delay time between the pulses, we show that this weak ferroelectric contribution is not stable and disappears with time. This might be due to orientation relaxation of the ferroelectric domains in the antiferroelectric matrix. Using the FORC measurements, we show that this ferroelectric contribution, visible at low fields, has a quite homogeneous hysteron distribution, corresponding to the observed broad distribution of the coercive field.

The high field PUND measurements reveal that the delay between pulses also affects the antiferroelectric to the ferroelectric phase transition fields which is higher for the first pulse of identical polarity, especially when the delay time is short. This indicates that the previously oppositely oriented ferroelectric phase hinders the antiferroelectric-ferroelectric transition. As the delay between pulses is getting longer, the difference between the switching and non-switching phase transition field vanishes.

The high field FORC measurements show that there exist a further ferroelectric contribution, which can be switched at fields of the order of the phase transition electric field. When the delay between the pulses increases, the magnitude of this ferroelectric peak decreases, again indicating that switching of this ferroelectric contribution is not

stable. This ferroelectric switching contribution, not visible on the $P(E)$ loops, shows the sensibility of the FORC method and its complementarity with the PUND measurements.

Data availability

The data that support the findings of this study are available from the corresponding author upon reasonable request.

Acknowledgments

This work has been performed with the means of the technological platform SMART SENSORS of the French region Pays de la Loire and with the means of the CERTeM (microelectronics technological research and development center) of French region Centre Val de Loire.

Conflict of interest

The authors declare that they have no known competing financial interests or personal relationships that could have appeared to influence the work reported in this paper.

References

[1] M. D. Coulibaly, C. Borderon, R. Renoud, H. W. Gundel, Enhancement of $PbZrO_3$ polarization using a ti seed layer for energy storage application, Thin Solid Films 716 (2020) 138432. doi:10.1016/j.tsf.2020.138432.
URL https://doi.org/10.1016/j.tsf.2020.138432

[2] M. Sharifzadeh Mirshekarloo, K. Yao, T. Sritharan, Large strain and high energy storage density in orthorhombic perovskite (pb0.97la0.02)(zr1-x-ySnxTiy)o3 antiferroelectric thin films, Applied Physics Letters 97 (14) (2010) 142902. doi:10.1063/1.3497193.
URL https://doi.org/10.1063/1.3497193

[3] C. Liu, S. X. Lin, M. H. Qin, X. B. Lu, X. S. Gao, M. Zeng, Q. L. Li, J.-M. Liu, Energy storage and polarization switching kinetics of (001)-oriented pb0.97la0.02(zr0.95ti0.05)o3 antiferroelectric thick films, Applied Physics Letters 108 (11) (2016) 112903. doi:10.1063/1.4944645.
URL https://doi.org/10.1063/1.4944645

[4] M. Sadl, O. Condurache, A. Bencan, M. Dragomir, U. Prah, B. Malic, M. Deluca, U. Eckstein, D. Hausmann, N. H. Khansur, K. G. Webber, H. Ursic, Energy-storage-efficient $0.9\,Pb(Mg_{1/3}\,Nb_{2/3})O_3 - 0.1\,PbTiO_3$ thick films integrated directly onto stainless steel, Acta Materialia 221 (2021) 117403. doi:https://doi.org/10.1016/j.actamat.2021.117403.

[5] X. Dai, J.-F. Li, D. Viehland, Weak ferroelectricity in antiferroelectric lead zirconate, Phys. Rev. B 51 (1995) 2651–2655. doi:10.1103/PhysRevB.51.2651.
URL https://link.aps.org/doi/10.1103/PhysRevB.51.2651

[6] K. Boldyreva, D. Bao, G. L. Rhun, L. Pintilie, M. Alexe, D. Hesse, Microstructure and electrical properties of $(120)_O$-oriented and of $(001)_O$-oriented epitaxial antiferroelectric $PbZrO_3$ thin films on (100) $SrTiO_3$ substrates covered with different oxide bottom electrodes, Journal of Applied Physics 102 (4) (2007) 044111. doi:10.1063/1.2769335.
URL https://doi.org/10.1063/1.2769335

[7] L. Pintilie, K. Boldyreva, M. Alexe, D. Hesse, Coexistence of ferroelectricity and antiferroelectricity in epitaxial $PbZrO_3$ films with different orientations, Journal of Applied Physics 103 (2) (2008) 024101. doi:10.1063/1.2831023.
URL https://doi.org/10.1063/1.2831023

[8] K. Nadaud, C. Borderon, R. Renoud, M. Bah, S. Ginestar, H. W. Gundel, Evidence of residual ferroelectric contribution in antiferroelectric lead-zirconate thin films by first-order reversal curves, Applied Physics Letters 118 (4) (2021) 042902. doi:10.1063/5.0043293.
URL https://doi.org/10.1063/5.0043293

[9] M. D. Coulibaly, C. Borderon, R. Renoud, H. W. Gundel, Effect of ferroelectric domain walls on the dielectric properties of $PbZrO_3$ thin films, Applied Physics Letters 117 (14) (2020) 142905. doi:10.1063/5.0017984.

[10] Z. Luo, X. Lou, F. Zhang, Y. Liu, D. Chang, C. Liu, Q. Liu, B. Dkhil, M. Zhang, X. Ren, H. He, Rayleigh-like nonlinear dielectric response and its evolution during electrical fatigue in antiferroelectric $(Pb, La)(Zr, Ti)O_3$ thin film, Applied Physics Letters 104 (14) (2014) 142904. doi:10.1063/1.4870992.

[11] W. J. Merz, Domain formation and domain wall motions in ferroelectric batio$_3$ single crystals, Phys. Rev. 95 (1954) 690–698. doi:10.1103/PhysRev.95.690.
URL https://link.aps.org/doi/10.1103/PhysRev.95.690

[12] C.-Y. Wang, C.-I. Wang, S.-H. Yi, T.-J. Chang, C.-Y. Chou, Y.-T. Yin, M. Shiojiri, M.-J. Chen, Paraelectric/antiferroelectric/ferroelectric phase transformation in as-deposited ZrO_2 thin films by the TiN capping engineering, Materials & Design 195 (2020) 109020. doi:10.1016/j.matdes.2020.109020.
URL https://doi.org/10.1016/j.matdes.2020.109020

[13] C. Mart, K. Kühnel, T. Kämpfe, S. Zybell, W. Weinreich, Ferroelectric and pyroelectric properties of polycrystalline la-doped HfO2 thin films, Applied Physics Letters 114 (10) (2019) 102903. doi:10.1063/1.5089821.
URL https://doi.org/10.1063/1.5089821

[14] K. Nadaud, M. Sadl, M. Bah, F. Levassort, H. Ursic, Effect of thermal annealing on dielectric and ferroelectric properties of aerosol-deposited $0.65\,Pb(Mg_{1/3}Nb_{2/3})O_3 - 0.35\,PbTiO_3$ thick films, Applied Physics Letters 120 (11) (2022) 112902. doi:10.1063/5.0087389.

[15] S. Martin, N. Baboux, D. Albertini, B. Gautier, A new technique based on current measurement for nanoscale ferroelectricity assessment: Nano-positive up negative down, Review of Scientific Instruments 88 (2) (2017) 023901. doi:10.1063/1.4974953.
URL https://doi.org/10.1063/1.4974953

[16] M. Si, X. Lyu, P. R. Shrestha, X. Sun, H. Wang, K. P. Cheung, P. D. Ye, Ultrafast measurements of polarization switching dynamics on ferroelectric and anti-ferroelectric hafnium zirconium oxide, Applied Physics Letters 115 (7) (2019) 072107. doi:10.1063/1.5098786.
URL https://doi.org/10.1063/1.5098786

[17] L. Mitoseriu, C. E. Ciomaga, V. Buscaglia, L. Stoleriu, D. Piazza, Hysteresis and tunability characteristics of $Ba(Zr,Ti)O_3$ ceramics described by first order reversal curves diagrams, Journal of the European Ceramic Society 27 (2007) 3723–3726. doi:10.1016/j.jeurceramsoc.2007.02.085.

[18] I. Fujii, E. Hong, S. Trolier-Mckinstry, Thickness Dependence of Dielectric Nonlinearity of Lead Zirconate Titanate Films, Ultrasonics, Ferroelectrics, and Frequency Control, IEEE Transactions on 57 (8) (2010) 1717–1723. doi:10.1109/TUFFC.2010.1610.

[19] L. Mitoseriu, L. Stoleriu, A. Stancu, C. Galassi, V. Buscaglia, First order reversal curves diagrams for describing ferroelectric switching characteristics, Processing and Application of Ceramics 3 (1-2) (2009) 3–7. doi:10.2298/pac0902003m.

[20] D. Ricinschi, A. Stancu, L. Mitoseriu, P. Postolache, M. Okuyama, First order reversal curves diagrams

applied for the ferroelectric systems, Journal of Optoelectronics and Advanced Materials 6 (2) (2004) 623–627.

[21] W. Zhu, I. Fujii, W. Ren, S. Trolier-McKinstry, Influence of Mn doping on domain wall motion in $Pb(Zr_{0.52}Ti_{0.48})O_3$ films, Journal of Applied Physics 109 (6) (2011) 064105. doi:10.1063/1.3552298.

[22] L. Stoleriu, A. Stancu, L. Mitoseriu, D. Piazza, C. Galassi, Analysis of switching properties of porous ferroelectric ceramics by means of first-order reversal curve diagrams, Phys. Rev. B 74 (17) (Nov. 2006). doi:10.1103/physrevb.74.174107.
URL https://doi.org/10.1103/physrevb.74.174107

[23] M. Hoffmann, T. Schenk, M. Pešić, U. Schroeder, T. Mikolajick, Insights into antiferroelectrics from first-order reversal curves, Applied Physics Letters 111 (18) (2017). doi:10.1063/1.5003612.
URL http://dx.doi.org/10.1063/1.5003612

[24] L. Cima, E. Laboure, P. Muralt, Characterization and model of ferroelectrics based on experimental preisach density, Review of Scientific Instruments 73 (10) (2002) 3546–3552. doi:10.1063/1.1505659.
URL https://doi.org/10.1063/1.1505659

[25] C. Borderon, R. Renoud, M. Ragheb, H. W. Gundel, Dielectric long time relaxation of domains walls in pbzrtio$_3$ thin films, Applied Physics Letters 104 (7) (2014) 072902. doi:10.1063/1.4866156.
URL http://scitation.aip.org/content/aip/journal/apl/104/7/10.1063/1.4866156

[26] W.-H. Chan, H. Chen, E. V. Colla, Temporal effect of low-temperature ferroelectric behaviors in pb0.97la0.02(zr0.60sn0.30ti0.10)o3 ceramics, Applied Physics Letters 82 (14) 2314–2316, publisher: American Institute of Physics. doi:10.1063/1.1565178.
URL https://aip.scitation.org/doi/abs/10.1063/1.1565178

[27] W. Chan, Z. K. Xu, J. Zhai, H. Chen, E. V. Colla, Temporal effects in dielectric properties of some antiferroelectric complex perovskites, AIP Conference Proceedings 677 (1) 10–19, publisher: American Institute of Physics. doi:10.1063/1.1609932.
URL https://aip.scitation.org/doi/abs/10.1063/1.1609932

[28] S. Yu, K. Yao, S. Shannigrahi, F. T. E. Hock, Effects of poly(ethylene glycol) additive molecular weight on the microstructure and properties of sol-gel-derived lead zirconate titanate thin films, Journal of Materials Research 18 (3) (2003) 737–741. doi:10.1557/JMR.2003.0100.

[29] G. Yi, M. Sayer, An acetic acid/water based sol-gel PZT process i: Modification of Zr and Ti alkoxides with acetic acid, Journal of Sol-Gel Science and Technology 6 (1) (1996) 65–74. doi:10.1007/bf00402590.
URL https://doi.org/10.1007/bf00402590

[30] K. Nadaud, C. Borderon, R. Renoud, M. Bah, S. Ginestar, H. W. Gundel, Dielectric, piezoelectric and electrostrictive properties of antiferroelectric lead-zirconate thin films, Journal of Alloys and Compounds 914 (2022) 165340. doi:10.1016/j.jallcom.2022.165340.
URL https://doi.org/10.1016/j.jallcom.2022.165340

[31] P. Ayyub, S. Chattopadhyay, R. Pinto, M. S. Multani, Ferroelectric behavior in thin films of antiferroelectric materials, Phys. Rev. B 57 (1998) R5559–R5562. doi:10.1103/PhysRevB.57.R5559.
URL https://link.aps.org/doi/10.1103/PhysRevB.57.R5559

[32] M.-H. Zhang, L. Fulanović, S. Egert, H. Ding, P. B. Groszewicz, H.-J. Kleebe, L. Molina-Luna, J. Koruza, Electric-field-induced antiferroelectric to ferroelectric phase transition in polycrystalline NaNbO3, Acta Materialia 200 (2020) 127–135. doi:10.1016/j.actamat.2020.09.002.
URL https://doi.org/10.1016/j.actamat.2020.09.002

[33] Y. Li, W. Cao, Q. Li, Q. Yan, J. Gao, F. Zhuo, X. Xi, Y. Zhang, X. Chu, Electric field induced metastable ferroelectric phase and its behavior in (Pb,La)(Zr,Sn,Ti)O_3 antiferroelectric single crystal near morphotropic phase boundary, Applied Physics Letters 104 (5) (2014) 052912. doi:10.1063/1.4864317.
URL https://doi.org/10.1063/1.4864317

[34] T. Yang, X. Yao, Metastable ferroelectric phase in lanthanum-doped lead zirconate titanate stannate antiferroelectric ceramics, Ceramics International 34 (4) (2008) 715–717. doi:10.1016/j.ceramint.2007.09.013.
URL https://doi.org/10.1016/j.ceramint.2007.09.013

[35] F. Zhuo, Q. Li, Y. Li, J. Gao, Q. Yan, Y. Zhang, X. Xi, X. Chu, W. Cao, Field induced phase transitions and energy harvesting performance of $(Pb, La)(Zr, Sn, Ti)O_3$ single crystal, Journal of Applied Physics 121 (6) (2017) 064104. doi:10.1063/1.4975786.

[36] J. Gao, Q. Li, Y. Li, F. Zhuo, Q. Yan, W. Cao, X. Xi, Y. Zhang, X. Chu, Electric field induced phase transition and domain structure evolution in $(Pb, La)(Zr, Sn, Ti)O_3$ single crystal, Applied Physics Letters 107 (7) (2015) 072909. doi:10.1063/1.4929463.

[37] J. Li, X. Su, J. Li, S. Qin, H.-H. Wu, D. Guo, Y. Su, L. Qiao, Y. Bai, Memory effect in antiferroelectrics: A systematic analysis on various electric hysteresis loops, Scripta Materialia 191 (2021) 143 – 148. doi:https://doi.org/10.1016/j.scriptamat.2020.09.033.
URL http://www.sciencedirect.com/science/article/pii/S1359646220306321

[38] G. Le Rhun, R. Bouregba, G. Poullain, Polarization loop deformations of an oxygen deficient $Pb(Zr_{0.25}Ti_{0.75})O_3$ ferroelectric thin film, Journal of Applied Physics 96 (10) (2004) 5712–5721. doi:10.1063/1.1789635.

[39] W. Wu, K. H. Wong, C. L. Choy, Interface-oxygen-loss-controlled voltage offsets in epitaxial $Pb(Zr_{0.52}Ti_{0.48})O_3$ thin-film capacitors with $La_{0.7}Sr_{0.3}MnO_3$ electrodes, Applied Physics Letters 85 (21) (2004) 5013–5015, publisher: American Institute of Physics. doi:10.1063/1.1827929.
URL http://aip.scitation.org/doi/10.1063/1.1827929